cmgh
CELLULAR AND MOLECULAR GASTROENTEROLOGY AND HEPATOLOGY

ORIGINAL RESEARCH

STING Activated Tumor-Intrinsic Type I Interferon Signaling Promotes CXCR3 Dependent Antitumor Immunity in Pancreatic Cancer

Emily P. Vonderhaar,[1,2,3] Nicholas S. Barnekow,[1,2] Donna McAllister,[1,2] Laura McOlash,[1,2] Mahmoud Abu Eid,[1,2] Matthew J. Riese,[1,2,3,4,5] Vera L. Tarakanova,[1,2] Bryon D. Johnson,[1,2,3] and Michael B. Dwinell[1,2,3,4,6]

[1]Department of Microbiology and Immunology, [2]Center for Immunology, [3]LaBahn Pancreatic Cancer Program, [4]Department of Medicine, [5]Versiti Blood Research Institute, and [6]Department of Surgery, Medical College of Wisconsin, Milwaukee, Wisconsin

SUMMARY

Our data demonstrate that pancreatic cancer cells actively signal broad antitumor immune responses through STING agonist induced type I IFN signaling and chemokine production that drive the infiltration and activation of cytolytic T cells in local and distant pancreatic tumors.

BACKGROUND & AIMS: Pancreatic ductal adenocarcinoma (PDA) is a lethal chemoresistant cancer that exhibits early metastatic spread. The highly immunosuppressive PDA tumor microenvironment renders patients resistant to emerging immune-targeted therapies. Building from our prior work, we evaluated stimulator of interferon genes (STING) agonist activation of PDA cell interferon-α/β-receptor (IFNAR) signaling in systemic antitumor immune responses.

METHODS: PDA cells were implanted subcutaneously to wild-type, IFNAR-, or CXCR3-knockout mice. Tumor growth was monitored, and immune responses were comprehensively profiled.

RESULTS: Human and mouse STING agonist ADU-S100 reduced local and distal tumor burden and activated systemic antitumor immune responses in PDA-bearing mice. Effector T-cell infiltration and inflammatory cytokine and chemokine production, including IFN-dependent CXCR3-agonist chemokines, were elevated, whereas suppressive immune populations were decreased in treated tumors. Intratumoral STING agonist treatment also generated inflammation in distal noninjected tumors and peripheral immune tissues. STING agonist treatment of type I IFN–responsive PDA tumors engrafted to IFNAR$^{-/-}$ recipient mice was sufficient to contract tumors and stimulate local and systemic T-cell activation. Tumor regression and CD8^{+} T-cell infiltration were abolished in PDA engrafted to CXCR3$^{-/-}$ mice treated with STING agonist.

CONCLUSIONS: These data indicate that STING agonists promote T-cell infiltration and counteract immune suppression in locally treated and distant tumors. Tumor-intrinsic type I IFN signaling initiated systemic STING-mediated antitumor inflammation and required CXCR3 expression. STING-mediated induction of systemic immune responses provides an approach to harness the immune system to treat primary and disseminated pancreatic cancers. *(Cell Mol Gastroenterol Hepatol 2021;12:41–58; https://doi.org/10.1016/j.jcmgh.2021.01.018)*

Keywords: Antitumor Immunity; Tumor Microenvironment; Flow Immunophenotyping; Tumor-Intrinsic IFNAR Signaling.

Pancreatic ductal adenocarcinoma (PDA) remains a highly fatal cancer, with poor responsiveness to chemotherapy.[1,2] Most patients present with distant metastases precluding surgical resection eligibility, the only current life-sparing intervention.[3] Conventional chemotherapy or radiotherapy strategies, alone or in combination, have shown modest benefits. Therapeutic resistance largely stems from the densely fibrotic, poorly vascularized, and immune-suppressed PDA tumor microenvironment.[4–6] Emerging strategies targeting the desmoplastic response or the pronounced immune suppression within the PDA tumor microenvironment have shown minimal improvement in patient outcomes.[7,8] The predominant immunotherapies currently in clinical use interfere with inhibitory checkpoint signaling by T cells and have shown some success in immunogenic tumors inherently abundant with tumor-specific T cells.[9] In contrast, PDA is largely a non-immunogenic tumor devoid of cytolytic tumor-reactive CD8^{+} T cells and rich in suppressive leukocyte populations within the tumor.[6,10–12] Immunogenic and non-immunogenic tumors evade antitumor immunity through different mechanisms, with immunogenic tumors largely inhibiting effector T-cell function, whereas non-immunogenic

Abbreviations used in this paper: **DMEM, Dulbecco modified Eagle medium; IFNAR, interferon-α/β-receptor; IRF3, interferon regulatory factor 3; PBS, phosphate-buffered saline; PDA, pancreatic ductal adenocarcinoma; RT-PCR, reverse transcriptase polymerase chain reaction; SD, standard deviation; SEM, standard error of the mean; STING, stimulator of interferon genes; TAM, tumor-associated macrophage; TBK1, TANK-binding kinase 1; TDLN, tumor-draining lymph node; TIL, tumor-infiltrating lymphocyte; Treg, regulatory T cell; type I IFN, type I interferon.**

Most current article

2352-345X
https://doi.org/10.1016/j.jcmgh.2021.01.018

tumors limit priming, activation, and/or infiltration of tumor-reactive T cells.[13] In patients with detectable anti-PDA T cells, effector lymphocytes are actively excluded from infiltrating the tumor parenchyma.[12,14] Thus, therapeutic strategies to increase both antitumor T-cell generation and infiltration into the primary tumor and disseminated disease sites may induce immune-mediated PDA tumor control.

Recent studies have identified the innate immune stimulator of interferon genes (STING) pathway in the generation of antitumor immune responses to immunogenic tumors.[15,16] Furthermore, therapeutic STING activation enhances preexisting antitumor immunity to eradicate local and distant immunogenic tumors in preclinical subcutaneous models.[17–19] Cyclic dinucleotides, produced by intracellular bacteria or endogenous cyclic guanosine monophosphate–adenosine monophosphate synthase action on cytosolic double-stranded DNA, bind to the STING receptor residing within the endoplasmic reticulum membrane.[20] Activated STING recruits TANK-binding kinase 1 (TBK1) to activate the transcription factor interferon regulatory factor 3 (IRF3), culminating in the expression of effector antiviral cytokines and chemokines, especially type I interferons (type I IFNs), IFNα and IFNβ, that signal through the ubiquitous type I IFN receptor (IFNAR).[21,22] Type I IFNs interfere with viral infection in part through induction of apoptosis and inhibition of cellular proliferation of infected cells.[23] IFNAR activation can also elicit tumor-intrinsic antiproliferative signaling.[24] Recently, type I IFN–induced transcriptional signatures were associated with immunogenic T cell-inflamed human melanoma tumors, demonstrating tumor-extrinsic antitumor effects of IFNAR.[25] Indeed, dendritic cell–mediated generation of tumor-specific $CD8^+$ T cells is dependent on IFNAR signaling in immunogenic tumor models.[25,26] In pancreatic cancer, type I IFN responses are thought to be actively repressed as a consequence of KRAS and MYC oncogene signaling.[27] The ability of STING agonist to generate widespread antitumor immunity against non-immunogenic pancreatic tumors through tumor-intrinsic or tumor-extrinsic type I IFN signaling could prove a powerful strategy to overcome oncogene enforced immune suppression and evasion.

We recently reported that intratumoral STING agonist monotherapy debulked singular subcutaneous murine PDA tumors by increasing the frequency of effector T cells and decreasing suppressive immune populations within tumors.[28] Importantly, tumor-reactive T cells were identified in the periphery of PDA-bearing mice after treatment, suggesting that locally administered STING agonists may promote systemic antitumor immunity.[28] Here, we investigated the ability of a clinically relevant STING agonist to elicit systemic adaptive immune responses in a non-immunogenic PDA tumor model and examine the role for PDA epithelial IFNAR in STING-induced tumor inflammation. We discovered that local STING activation altered the magnitude of tumor burden and quality of the immune landscape at both local and distant tumor sites. Importantly, IFNAR signaling by pancreatic tumor cells was sufficient to initiate STING agonist-mediated immune responses. Furthermore, STING activation induced the expression of IFN-dependent CXCR3-attracting chemokines. Our data show that the antitumor effects were dependent on CXCR3 expression, demonstrating the critical role for CXCR3 in STING agonist-induced tumor inflammation and tumor regression. The ability of STING agonist to stimulate local and systemic immune activation suggests a potential clinical avenue for treating patients with localized resectable or disseminated unresectable pancreatic tumors.

Results

STING Agonist ADU-S100 Reduces Tumor Burden and Inflames PDA Tumors

Activation of the antiviral innate immune receptor STING may be exploited therapeutically to promote antitumor immunity.[29] We recently demonstrated that DMXAA, a flavonoid-like molecule specific for mouse STING,[30,31] effectively contracts PDA tumors in a $CD8^+$ T cell-dependent manner.[28] Because DMXAA cannot activate human STING agonists and failed in clinical trials, we investigated the response of PDA to a Food and Drug Administration–cleared agonist, ADU-S100 (S100), a mixed [2,3]-linkage analog of cyclic-di-adenosine monophosphate that activates each of the 5 allelic variants of human STING that can also bind mouse STING.[17] Murine KPC cell–engrafted tumors faithfully recapitulate human pancreatic cancers, including the stromal desmoplastic reaction and immunosuppression.[4,32] To determine the efficacy of S100 in pancreatic cancer, mice were engrafted with KPC cells and treated as outlined in Figure 1*A*. S100 was as effective as DMXAA at reducing tumor burden (Figure 1*B*), with doses as low as 10 μg inhibiting tumor progression (Figure 1*C*). As shown in Figure 1*D*, S100-treated mice exhibited a median survival of 56 days, 2.5 times longer than that of control mice.

Subsequently, we assessed the ability of antitumor doses of S100 to promote immune activation. Immunophenotyping of pancreatic tumors by flow cytometry using gating strategies illustrated in Figure 1*E* and *F* revealed that S100 was as effective as DMXAA in shifting tumors to a more immunogenic phenotype (Figure 1*G*). Critically, S100 increased the $CD8^+$ T cell frequency of total T cells, and ratio of cytolytic $CD8^+$ to helper $CD4^+$ T cells (Figure 1*G*) within diminishing pancreatic tumors compared with untreated tumors. Moreover, $CD8^+$ T cells within the treated tumors demonstrated increased granzyme B expression and elevated frequency of chemokine receptor CXCR3-expressing cells (Figure 1*G*). Levels of $CD4^+Foxp3^+$ regulatory T cells (Tregs) were decreased, with a concomitant diminished ratio of suppressive $Foxp3^+$ to effector $CD8^+$ T lymphocytes upon STING agonist treatment (Figure 1*G*). The response was not limited to T-cell infiltration and activation because S100 simultaneously decreased levels of $CD45^+Ly6C^-MHCII^+CD11b^+F4/80^+$ tumor-associated macrophages (TAMs) within the tumor (Figure 1*G*). Furthermore, the remaining TAMs were increasingly repolarized to a more inflammatory type, as evidenced by a reduced level of CD206 expression, a marker of suppressive-type macrophages (Figure 1*G*).

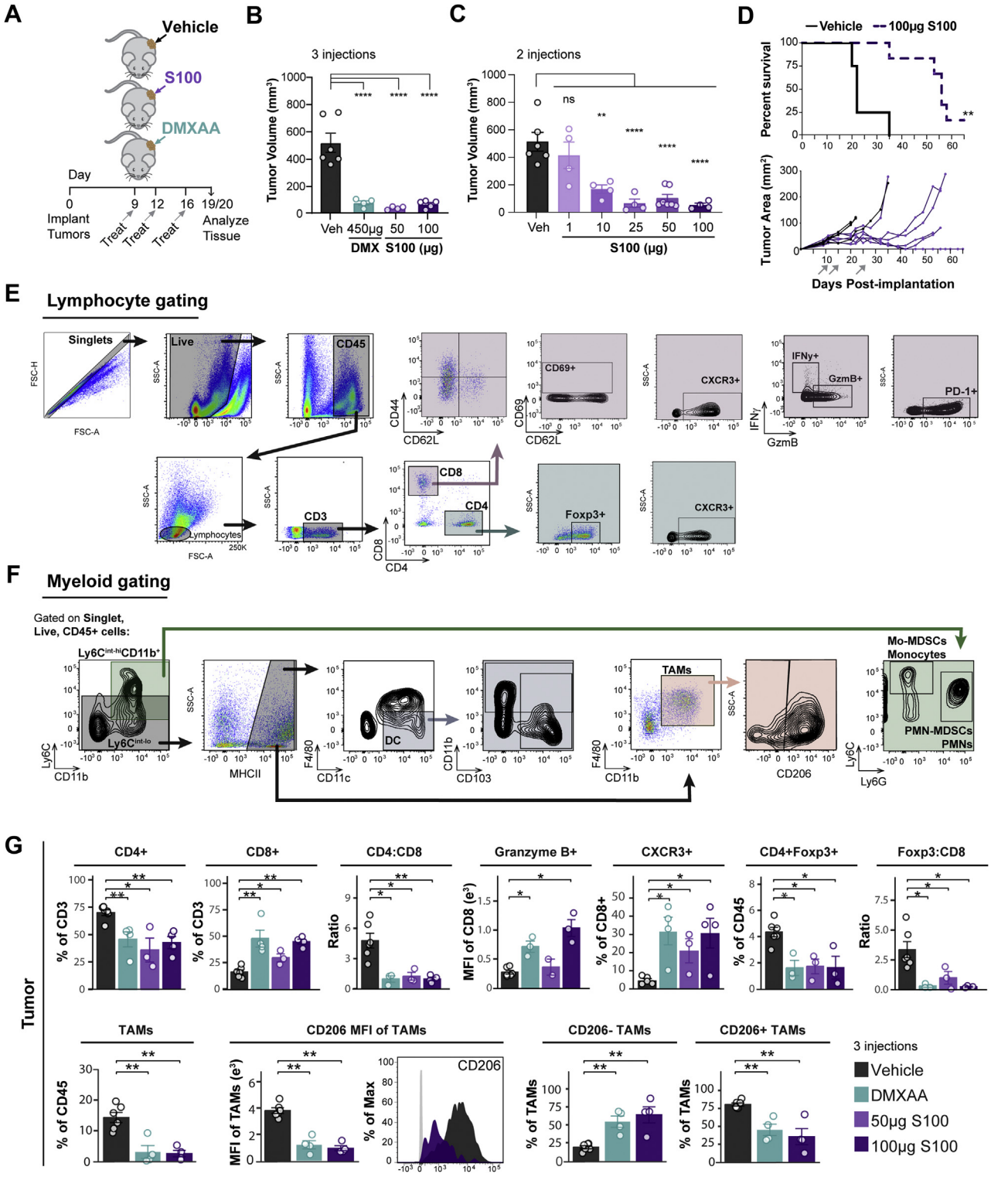

Figure 1. ADU-S100 STING agonist reduces tumor burden and activates the pancreatic cancer immune microenvironment. (*A*) Schematic of experimental treatment plan. C57BL/6 mice were implanted into a single-flank with KPC1242 cells and treated with 2 or 3 intratumoral injections of 450 μg DMXAA (*teal*), 1 μg, 10 μg, 25 μg, or 100 μg ADU-S100 (S100, *purple*), or vehicle control (*black*). (*B*) Tumors were harvested after 3 injections and measured ex vivo. (*C*) Tumor volume at study end from mice treated twice with dose titration of S100. (*D*) Kaplan-Meier survival curve with log-rank test analysis (*top panel*) and individual animal PDA tumor area (*bottom panel*) over time. *Gray arrows* indicate treatment on days 11, 15, and 25. n = 4 (control), n = 6 (S100). (*E* and *F*) Representative gating strategies for flow cytometric analysis of lymphocyte populations (*E*) and myeloid populations (*F*). *Shaded regions* indicate selected cell populations in gating scheme. (*G*) Tumors from (*B*) were analyzed by flow cytometry. Error bars represent mean ± standard error of the mean (SEM). n = 3–6. FC, fold-change; MFI, median fluorescence intensity; ns, not significant. *$P < .05$, **$P < .01$, ***$P < .001$, ****$P < .0001$.

Next, an unbiased multiplex cytokine array of whole tumor homogenates evaluated immune mediator levels within treated tumors. Inflammatory cytokines interleukin 6, tumor necrosis factor, and IFNγ were significantly increased in S100-treated tumors (Figure 2*A*). Moreover, monocyte, neutrophil, and T cell–attracting chemokines were significantly elevated in response to S100 treatment (Figure 2*A*). Notably, S100 stimulated the production of IFN-regulated chemokines CXCL9 and CXCL10 (Figure 2*A*), with concentrations within the physiological range for stimulating trafficking of activated T cells (Figure 2*B*). Thus, intratumoral S100 shifts PDA tumors from immune-tolerant to immune-permissive, impacting both T cells and myeloid cell subsets to reverse immune suppression typical of pancreatic cancers. Together, these data indicate that S100, a compound currently enrolled in clinical trials for treatment of superficial tumors (NCT02675439, NCT03172936, NCT03937141), has potent antitumor properties against PDA.

Antitumor Effects of STING Agonist in Local Treated and Distal Untreated PDA

STING agonists are typically administered directly into tumors in an effort to avoid off-tumor immunotoxicity, limiting the potential clinical utility of STING agonists in deep tumors like PDA.[33] We previously observed elevated tumor-reactive T cells in the periphery of PDA-bearing mice treated with DMXAA, suggesting that intratumoral STING agonist may promote systemic antitumor immunity.[28] To test the potential for STING agonist to inhibit tumor growth in local injected as well as distal non-injected tumors, a dual flank tumor model in which syngeneic mice were synchronously implanted with KPC cells was created. The flank with the larger number of implanted cells was directly treated and was defined as the "injected" tumor, whereas fewer cells engrafted to the "contralateral" flank served as a surrogate disseminated tumor and did not receive direct treatment (Figure 3*A*). For these studies, we used a DMXAA dosing regimen that generated antitumor T cells in our initial report.[28] The median survival of mice treated with STING agonist was 48% longer than in control mice (Figure 3*B*), with increased survival mirrored by significantly decreased tumor size in both the injected and the contralateral tumor (Figure 3*C*). Tumor regression of the contralateral tumor was delayed relative to that of the injected tumor (Figure 3*D*), as might be expected from STING-generated antitumor T-cell responses.

Because of our previous report showing that DMXAA does not directly inhibit PDA growth or induce apoptosis,[28] we next investigated whether the decreased size of non-injected tumors corresponded with increased tumor microenvironment inflammation. As predicted, DMXAA-injected tumors had increased frequencies of $CD8^+$ T cells, increased levels of $CD8^+$ T-cell granzyme B and CXCR3 expression, decreased frequency of Tregs, and decreased Foxp3:CD8 ratio (Figure 4*A*). Notably, the cellular landscape within noninjected contralateral tumors of STING agonist-treated mice paralleled that of the injected tumors, with similar changes and trends in lymphocyte populations (Figure 4*B*). $CD8^+$ tumor-infiltrating lymphocytes from both injected and contralateral tumors recognized and induced killing of PDA tumor cells (Figure 4*C*), confirming that STING treatment induced tumor-specific T-cell activation rather than merely generalized inflammation. STING agonist also remodeled the myeloid compartment at both sites (Figure 4*D* and *E*). TAMs comprised less of the immune infiltrate, with diminished CD206 expression observed in both injected and contralateral tumors of DMXAA-treated animals (Figure 4*D* and *E*). The composition of natural killer cells, B cells ($CD19^+$), monocytes or monocytic-myeloid derived suppressor cells ($CD45^+CD11b^+$, $Ly6C^{hi}$, $Ly6G^{lo}$), and neutrophils or polymorphonuclear-myeloid derived suppressor cells ($CD45^+CD11b^+$, $Ly6C^{int}$, $Ly6G^{hi}$) in injected or contralateral tumors was little changed by treatment (Figure 4*F*). These data indicate that intratumoral STING agonist treatment induces antitumor effects in local and distal PDA tumors, with concordant inflammation of the immune microenvironment and activation of tumor antigen-specific T cells.

Intratumoral STING Agonists Stimulate Local and Global Immune Responses

To reinforce the potential systemic effects of STING agonists, we next measured the ability of S100 to modulate local as well as distant immune responses. After S100 treatment injected tumors uniformly shrank (Figure 5*A*–*C*). In contralateral tumors of S100-treated mice, PDA growth was also inhibited, and the tumor microenvironment showed an increased frequency of $CD8^+$ T cells and decreased ratio of Treg-to-$CD8^+$ T cells (Figure 5*A*–*D*). Moreover, tumor-infiltrating T cells were activated with elevated levels of IFNγ, granzyme B, and CD69, and there was a decreased proportion of CD62L-expressing cells (Figure 5*D*). PD-1^+CD8^+ T cells were increased, as expected from the increased production of IFNγ[34] (Figure 5*D*). As seen with DMXAA, S100 treatment effects were not restricted to T cells because there was a decreased frequency of TAMs within the total $CD45^+$ immune infiltrate and decreased TAM CD206 expression, consistent with a likely shift from suppressive to inflammatory macrophages (Figure 5*D*).

Although most PDA tumors are immune suppressed, the presence of tumor antigen-specific T cells in the tumor and periphery has been linked to long-term PDA survival, demonstrating the importance of generating widespread immunity.[35] Thus, we examined whether the immune-stimulating effects of STING agonist were restricted to tumors, as may be expected if the contralateral tumor response solely reflected diffusion of drug into the site, or were more widespread, suggesting the development of systemic antitumor immunity. To this end, the spleen and tumor-draining lymph nodes (TDLNs) from injected and contralateral tumors were collected and processed for flow cytometry. The relative abundance of $CD4^+$ and $CD8^+$ T cells in these lymphoid tissues was unaltered by S100

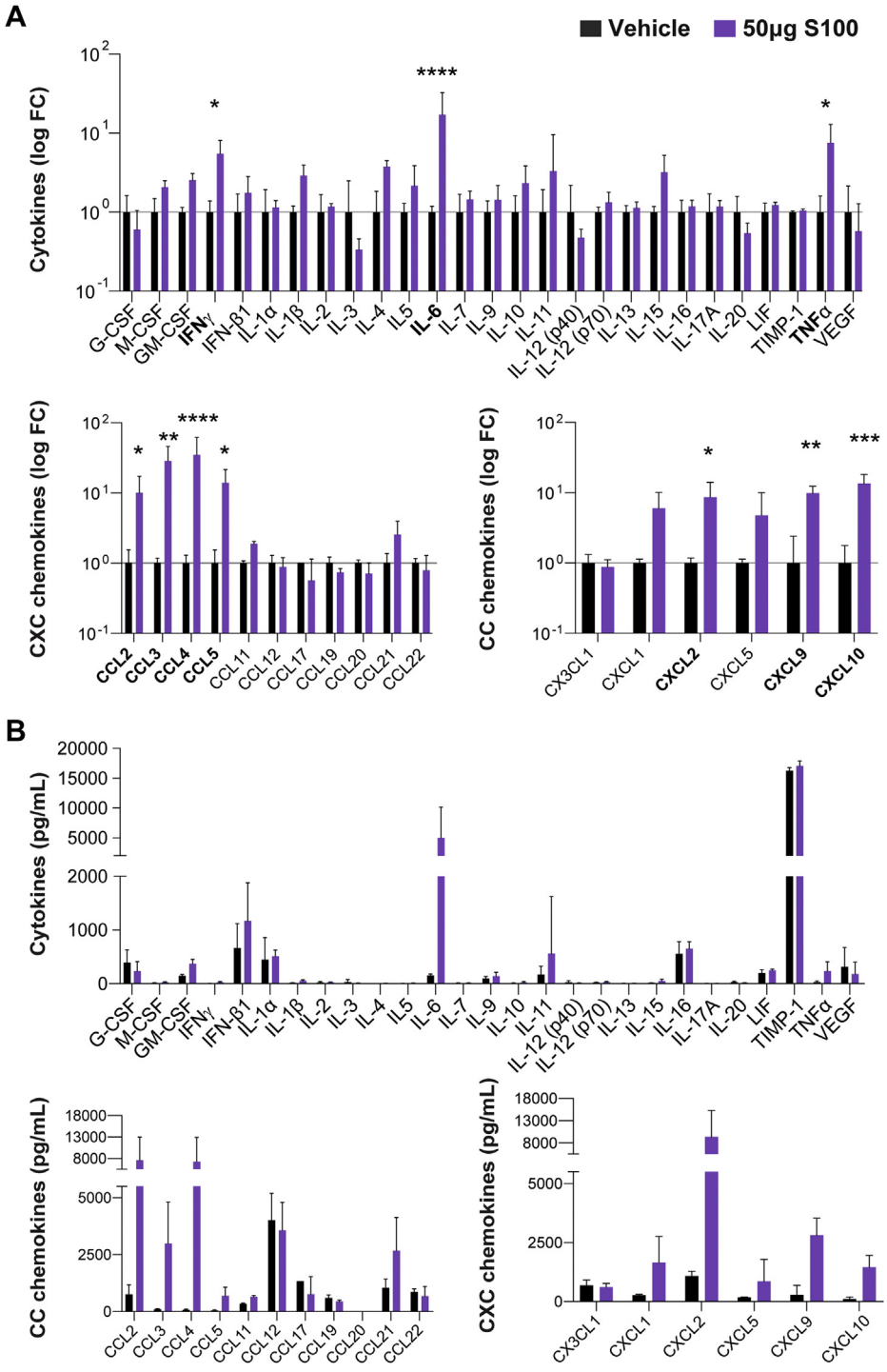

Figure 2. Unbiased screen of immune messengers in ADU-S100 or vehicle-treated pancreatic tumors. (*A*) Fold change in concentration of secreted cytokines (*top panel*) and chemokines (*bottom panels*) from S100-treated tumors relative to mean of control tumors in a single-flank PDA-bearing mouse model after 2 treatments was calculated and graphed on a log-scale. Proteins in *bold font* were significantly increased. (*B*) Quantification of secreted cytokine (*top panel*) and chemokine (*bottom panels*) concentrations from treated and untreated tumors shown as percent change (*A*). Error bars represent mean ± standard deviation (SD). n = 3 (control), n = 4 (S100) from one independent experiment. FC, fold change. **P* < .05, ***P* < .01, ****P* < .001, *****P* < .0001.

treatment (Figure 5*E*). However, the percent of $CD8^+$ T cells expressing CD62L decreased, and those expressing CD69, CD44, and granzyme B^+ increased in these tissues of S100-treated mice (Figure 5*F* and *G*). Furthermore, IFNγ producing $CD8^+$ T cells were significantly increased in the spleen and trended higher in TDLNs (Figure 5*F* and *G*). Consistent with S100-induced stimulation of an activated T-cell phenotype, the percent of $CD8^+$ T cells expressing CXCR3 was also elevated at all sites (Figure 5*F* and *G*). The global and consistent immune response in injected tumors, distal tumors, and peripheral immune tissues illustrates the power of S100 to induce systemic immune responses reflective of adaptive antitumor immune involvement.

Tumor-Intrinsic Type I IFN Signaling Drives Antitumor Effects of STING Agonist

Epithelial cells act as immune sentinels, but the contribution of PDA epithelial cell-intrinsic IFNAR signaling in STING-activated immune responses remains to be

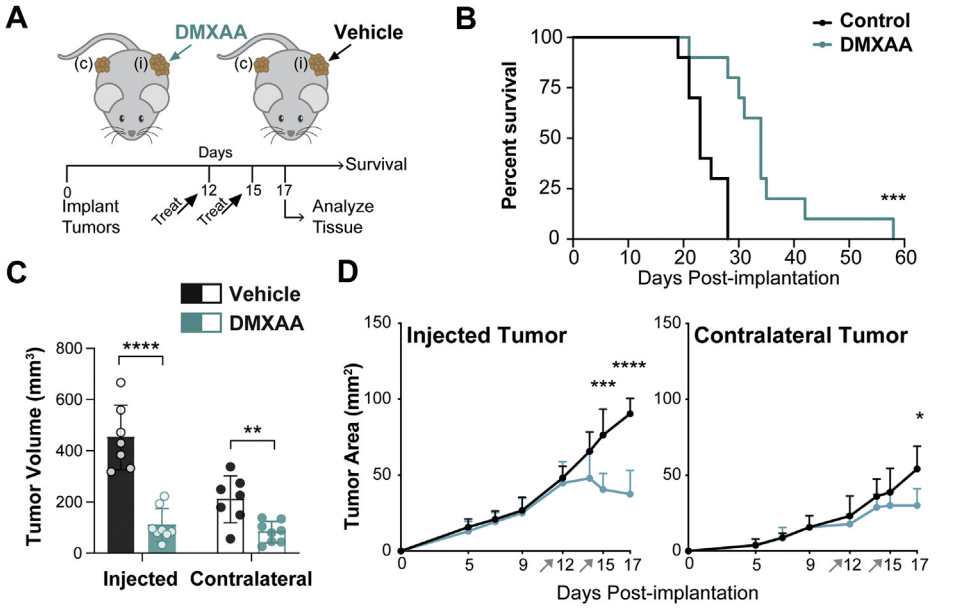

Figure 3. DMXAA STING agonist effects on tumor progression, survival, and size of primary and distal pancreatic tumors. (*A*) Mice were synchronously implanted onto each flank with KPC1242 cells. Injected tumors treated with 2 intratumoral injections of 450 μg DMXAA or vehicle control, whereas contralateral tumors were untreated. (*B*) Kaplan-Meier survival curve, log-rank (Mantel-Cox) test used to compare groups. (*C*) Tumor volume at harvest. (*D*) PDA tumor area over time in injected and contralateral flank tumors. Error bars represent mean ± SEM (*C*) or mean ± SD (*D*). n = 10 (*B*) and n = 7–9 (*C* and *D*) from 2 independent experiments. *$P < .05$, ***$P < .001$, ****$P < .0001$.

elucidated. To interrogate the role for tumor-intrinsic STING-IFNAR pathway signaling in PDA, cells were engrafted to IFNAR$^{-/-}$ or wild-type mice and treated with DMXAA or vehicle control. We verified STING mRNA expression in several murine PDA cell lines including engrafted KPC1242 cells (Figure 6*A*) and confirmed surface IFNAR expression by these cells using flow cytometry (Figure 6*B*). Importantly, DMXAA stimulated the production of inflammatory cytokines and chemokines across distinct PDA cell lines, verifying intact STING signaling by PDA cells (Figure 6*C*–*E*). Furthermore, STING agonist increased expression of *Mx1* and *Mx2,* two cardinal type I IFN–stimulated genes and sensitive indicators of IFNAR signaling, measured by semi-quantitative reverse transcriptase polymerase chain reaction (RT-PCR) analyses (Figure 6*F*).

Mice were treated as outlined in Figure 7*A.* The absence of IFNAR expression in knockout mice was validated (Figure 7*B*). After intratumoral STING agonist therapy, tumor size was reduced in both wild-type and IFNAR$^{-/-}$ mice (Figure 7*C*). The strong ablation of STING agonist-treated PDA tumors in IFNAR$^{-/-}$ mice was unexpected because prior reports in B16.F10 melanoma, a more immunogenic tumor, showed a lack of response to STING agonist treatment,[17] a finding we confirmed (Figure 7*D*). Our data suggest that epithelial tumor-intrinsic IFNAR signaling plays a role in STING-mediated antitumor responses in PDA.

Because STING agonist increased IFNβ and *Mx1* and *Mx2* expression by PDA cells, we profiled the immune microenvironment to determine the ability for tumor-intrinsic type I IFN-IFNAR signaling to inflame tumors after STING treatment. As shown in Figure 7*E*, STING agonist elevated the frequency of CD8$^+$ T cells and significantly increased levels of CXCR3-expressing CD8$^+$ T cells in IFNAR$^{-/-}$ recipient mice. Moreover, Foxp3$^+$ Treg to CD8$^+$ T-cell ratio and levels of suppressive CD206$^+$ TAMs were decreased in both knockout and wild-type mice (Figure 7*E*). Systemic immune responses evaluated in TDLNs and spleen revealed that the CD4$^+$ to CD8$^+$ T-cell ratio was unaffected by STING activation or IFNAR expression. In contrast, the percent CD8$^+$ T cells expressing CXCR3 increased in both TDLNs and spleen independent of IFNAR expression (Figure 7*F* and *G*). The extent to which CXCR3$^+$CD8$^+$ T cells in the periphery were increased by DMXAA was dependent on IFNAR, whereas those infiltrating the tumor were not (Figure 7*F* and *G*). These findings contrast with prior work in immunogenic tumors such as melanoma in which STING agonist responses required type I IFN receptor signaling by dendritic cells.[15,17,25,26,36,37] Taken together, our data from PDA indicate that tumor-intrinsic IFNAR signaling provides a sufficient immune activating signal within the tumor microenvironment to provoke STING agonist-induced immune responses within the tumor and more broadly in draining lymph nodes and spleen.

STING Agonist Effects on PDA Tumors Require T Cell CXCR3 Expression

CXCR3 is a chemokine receptor expressed on activated effector T cells that directs migration toward increasing concentration gradients of its ligands CXCL9 and CXCL10. Chemotactic migration requires the gradient be established from within the tumor to ensure robust tumor infiltration by T cells. We have shown that STING agonist potently increases production of type I IFN–regulated chemokines CXCL9 and CXCL10 in PDA tumors (Figure 2*A*). STING-stimulated PDA epithelial cells contributed to chemokine production directly, suggesting an autocrine type I IFN feedback loop in these IFNAR-expressing cancer cells (Figure 6*D* and *E*). Furthermore, STING agonist treatment of PDA tumors increased levels of CXCR3-expressing T cells within the tumor, lymph node, and spleen (Figure 7*E*–*G*). These data implicate the CXCR3-CXCL9/10 pathway in the

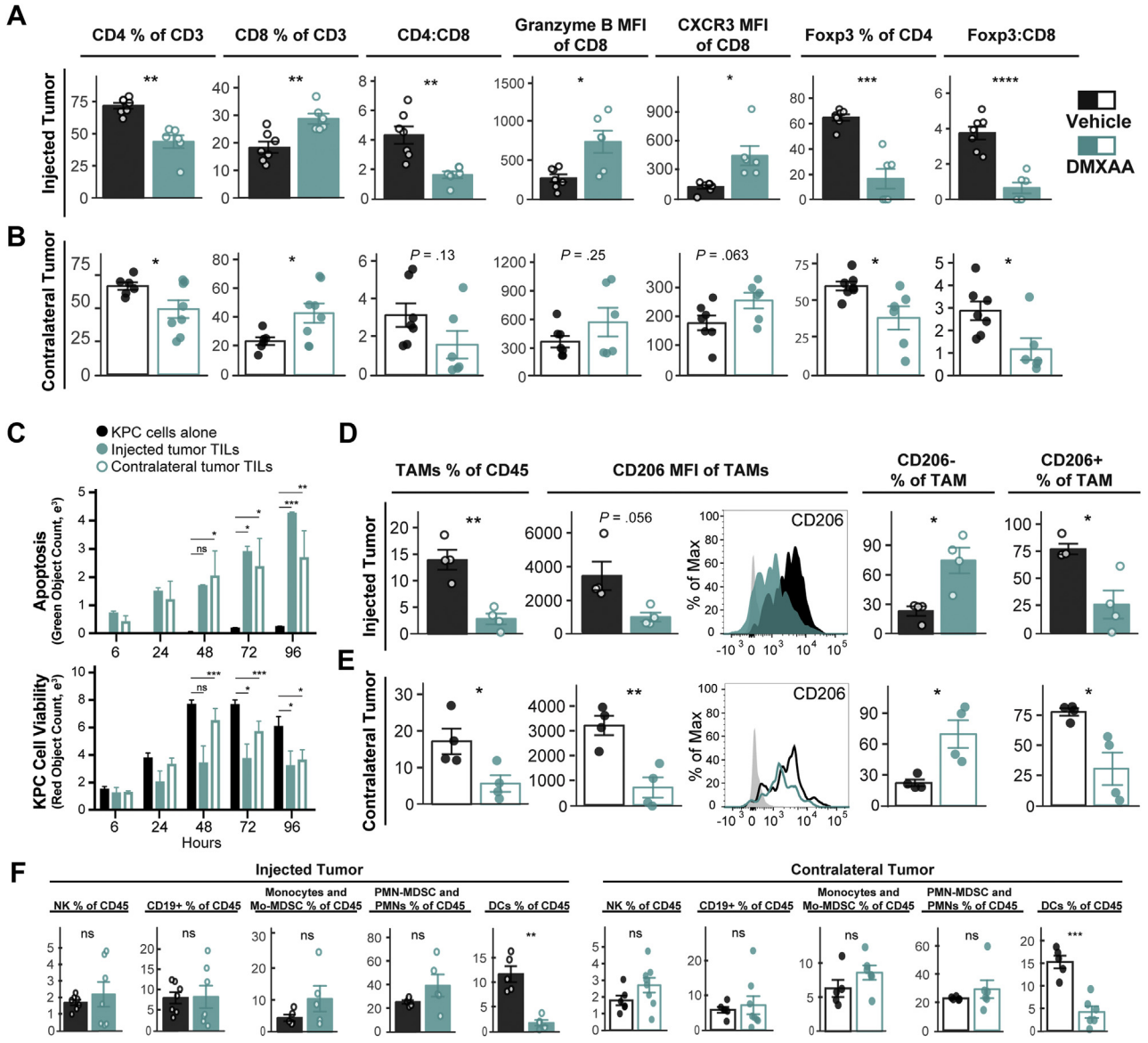

Figure 4. Local STING treatment stimulates widespread immune responses. Mice bearing dual-flank KPC tumors were treated intratumorally into a single-flank with 450 μg DMXAA (*teal*) or vehicle control (*black*). Tumors were harvested for flow cytometric analysis 2 days after second treatment. Lymphocytes were analyzed from injected (*A*) and contralateral (*B*) tumors. *Left to right*: $CD4^+$ and $CD8^+$ cell frequency of all tumor-infiltrating T cells, CD4:CD8 T-cell ratio, expression of granzyme B and CXCR3 within the $CD8^+$ cell compartment, and suppressive Tregs ($Foxp3^+$) frequency of $CD4^+$ T cells, $Foxp3^+$ to $CD8^+$ cell ratio. (*C*) KPC1242-nuclear red cell killing by $CD8^+$ TILs isolated and expanded from injected or contralateral tumors, and KPC1242-nuclear red cells alone in culture as control (*black bars*). Green object fluorescent count represents apoptosis (*top*), and red object count represents KPC cell viability (*bottom*). (*D* and *E*) Myeloid populations were analyzed from injected (*D*) and contralateral (*E*) tumors. *Left to right*: $CD45^+Ly6C^-MHCII^+CD11b^+F4/80^+$ TAMs, expression of CD206 on TAMs, TAMs lacking CD206 expression, and TAMs expressing CD206. Shown is a representative histogram of CD206 expression; *gray-filled curve* is unstained control. (*F*) Natural killer (NK) cells, B cells ($CD19^+$), monocytic-myeloid derived suppressor cells (Mo-MDSCs) or monocytes ($CD45^+CD11b^+$, $Ly6C^{hi}$, $Ly6G^{lo}$), polymorphonuclear cells (PMN) or PMN-MDSCs ($CD45^+CD11b^+$, $Ly6C^{int}$, $Ly6G^{hi}$), and dendritic cells (DCs; $CD45^+MHCII^+CD11c^+F4/80^{lo}$) were analyzed in injected (*left panel*) or contralateral (*right panel*) tumors. Error bars represent mean ± SEM. n = 5–6. MFI, median fluorescence intensity; ns, not significant. $^*P < .05$, $^{**}P < .01$, $^{***}P < .001$, $^{****}P < .0001$.

response of PDA tumors to STING agonist. We therefore tested the requirement for CXCR3 in STING-mediated ablation of PDA tumors and infiltration of cytotoxic T lymphocytes by treating PDA-engrafted wild-type or $CXCR3^{-/-}$ mice with DMXAA or vehicle control (Figure 8*A*). Absence of CXCR3 expression in knockout mice was validated (Figure 8*B* and *C*) and confirmed mouse PDA cells lacked expression of the chemokine receptor in agreement with our prior reports of human epithelial tissues (Figure 8*B*).[38,39] In contrast to the decrease in tumor size in $IFNAR^{-/-}$ and wild-

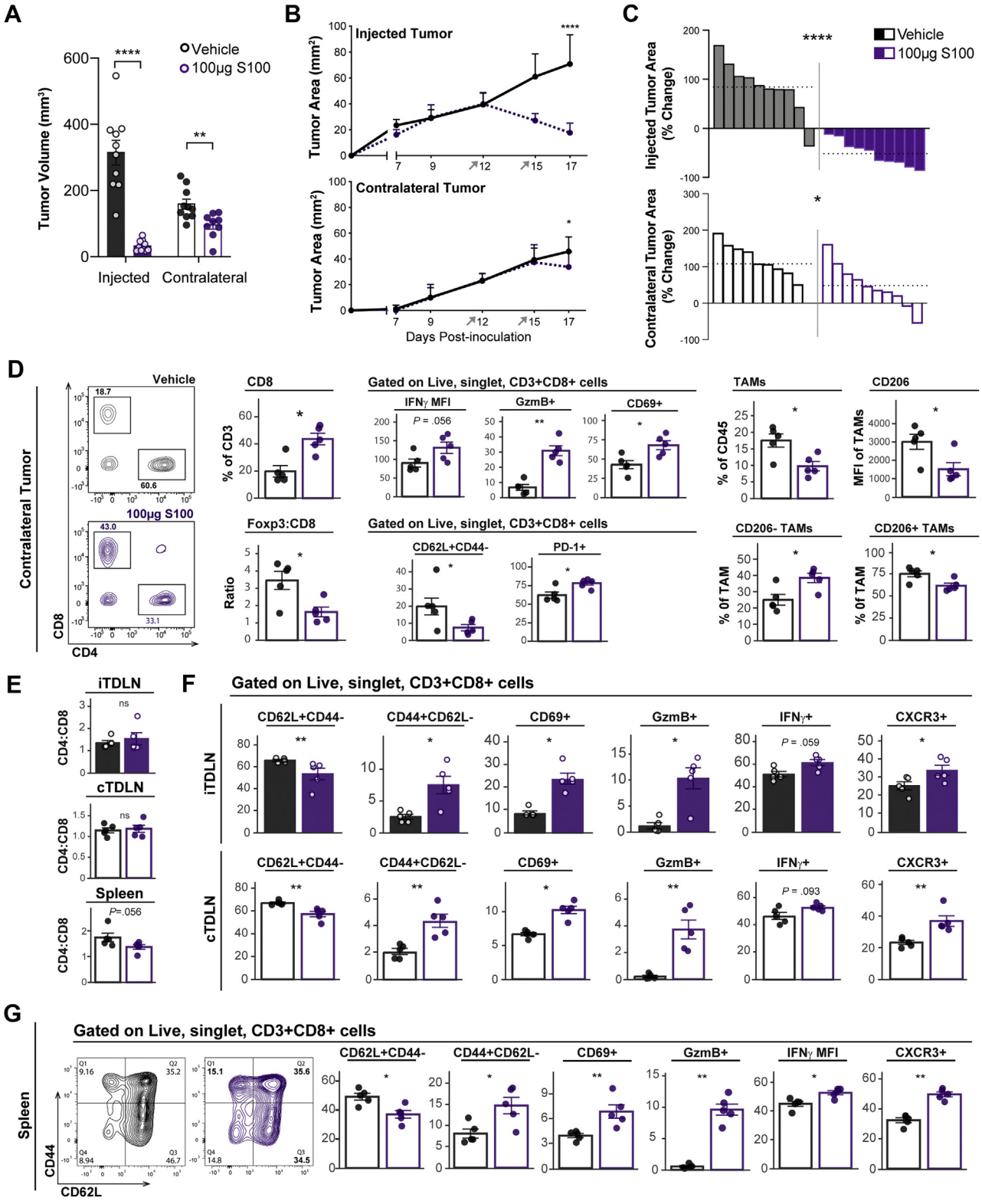

type engrafted mice, there was no effect of STING agonist on tumor volume in CXCR3$^{-/-}$ mice (Figure 8*D*). Furthermore, tumor inflammation, measured by total CD45^{+} leukocytes, and infiltration of cytolytic CD8^{+} T cells were unchanged with treatment in PDA-bearing CXCR3$^{-/-}$ mice (Figure 8*E* and *F*). Levels of CD3^{+} and CD8^{+} T cells in the spleen were unaffected by DMXAA treatment or expression of CXCR3 (Figure 8*G-I*). Likewise, lack of CXCR3 expression did not impact expression of CCR5, another chemokine receptor expressed on activated T cells (Figure 8*J*). Taken together, these data indicate that the full antitumor effects of STING agonists rely on expression of the T cell–trafficking

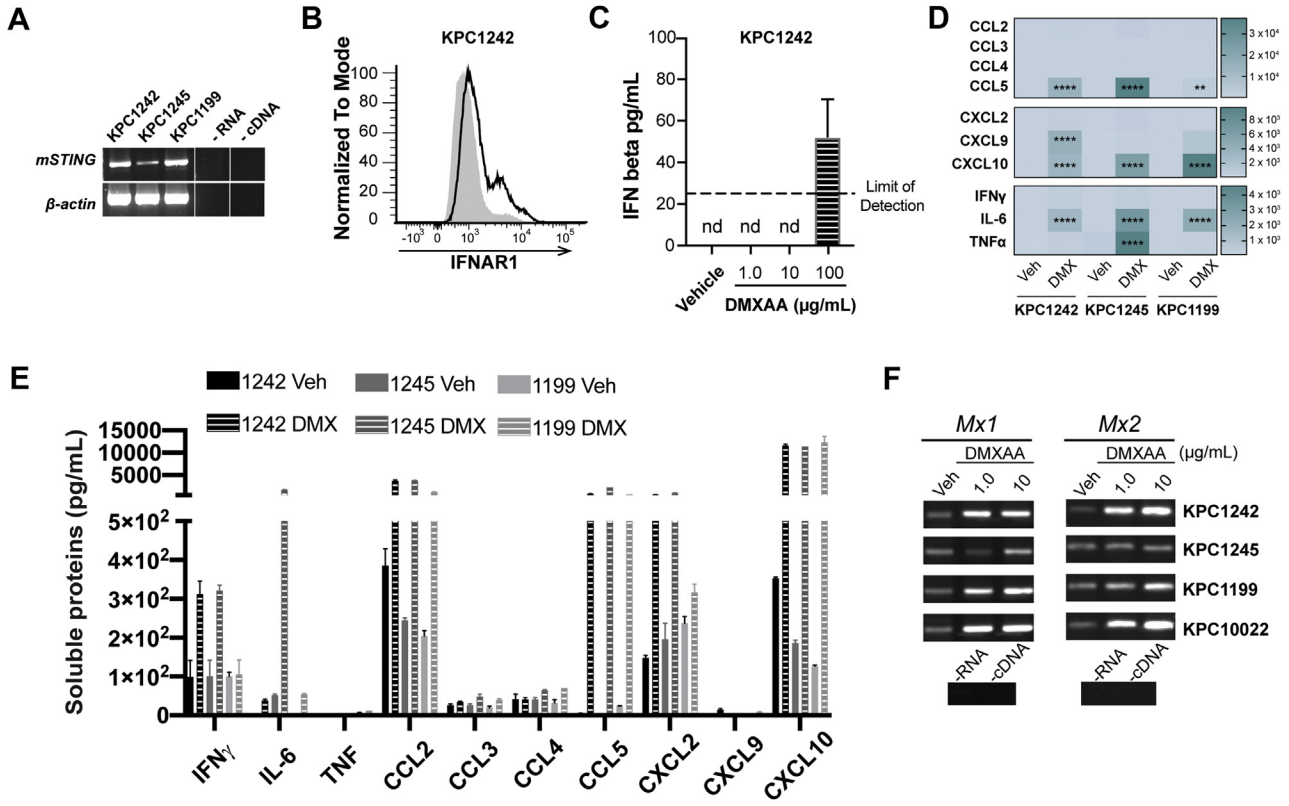

Figure 6. STING and IFNAR signaling by pancreatic cancer cells. (*A*) mRNA expression of *mSting* or *β-actin* control in 3 distinct mouse PDA cell lines. (*B*) Surface expression of IFNAR1 on KPC1242 cells (*dark line*) relative to isotype control (*gray-filled curve*). (*C*) IFNβ secretion by KPC1242 cells treated 24 hours with DMXAA. (*D* and *E*) Soluble proteins were measured in supernatant of mouse PDA cell lines treated with vehicle control or 100 μg DMXAA for 24 hours. Heatmap of the average fold-change levels of secreted proteins in DMXAA groups compared with control (*D*) and quantification of production (*E*). (*F*) mRNA from murine PDA cell lines stimulated 8 hours with 1 or 10 μg/mL DMXAA was reverse transcribed and then analyzed by semiquantitative PCR for *Mx1* and *Mx2* IFN-stimulated genes. Error bars represent mean ± SEM. ns, not significant. $^{**}P < .01$, $^{****}P < .0001$.

chemokine receptor CXCR3 and support a model in which tumor-intrinsic IFNAR signaling and T cell–attracting chemokine production drive tumor inflammation in immune suppressed pancreatic cancer.

Discussion

The majority of pancreatic cancer patients are diagnosed with unresectable disseminated disease and have limited therapeutic options. In this study, the ability of STING agonist to elicit widespread antitumor responses in an immune suppressed pancreatic cancer model was investigated. We demonstrated that STING agonists potently inhibited tumor progression and improved survival in PDA-bearing mice. DMXAA and human-targeted ADU-S100 robustly converted the immunologically inert PDA tumor into an immunogenic, inflamed tumor with abundant CXCR3-expressing cytotoxic T lymphocytes and diminished populations of suppressive myeloid and regulatory T cells. Moreover, the reinvigoration of the immunologic landscape within the tumor directly injected with STING agonist was mirrored in distal, noninjected tumors, implicating STING signaling in the development of systemic antitumor immune responses. Analysis of soluble factors

Figure 5. (***See previous page***). **ADU-S100 STING agonist inhibits pancreatic cancer growth and inflames distal untreated tumors.** Mice were synchronously implanted with dual-flank KPC tumors and treated twice with 100 μg S100 (*purple*) or vehicle control (*black*) injected to a single-flank. Tumors were harvested for flow cytometric analysis 2 days after second treatment. (*A*) Injected and contralateral tumor volume at study end. (*B*) Tumor growth kinetics of injected (*top*) and contralateral (*bottom*) tumors. (*C*) Waterfall plot of percent change in tumor area from day 12, before first treatment, to endpoint; each bar represents an individual mouse. *Dotted horizontal lines* represent the mean of each group. (*D*) Cell frequencies and phenotypes were analyzed in contralateral tumors. Representative $CD4^+$-by-$CD8^+$ T cell contour plot. (*E–G*) Cellular composition of the injected (iTDLNs) and contralateral (cTDLNs) tumors and within the spleen. Ratio of CD4:CD8 cells in these lymphoid tissues (*E*). Phenotype of $CD8^+$cells measured by CD62L, CD69, CD44, GzmB, IFNγ, and CXCR3 expression in TDLNs (*F*) and spleen (*G*). Error bars represent mean ± SEM (*A*, *D*, and *E*) or mean ± SD (*B*). n = 10 from 2 independent experiments (*A–C*), n = 5 (*D* and *E*). ns, not significant. $^{*}P < .05$, $^{**}P < .01$, $^{***}P < .001$, $^{****}P < .0001$. GzmB, granzyme B; MFI, median fluorescence intensity.

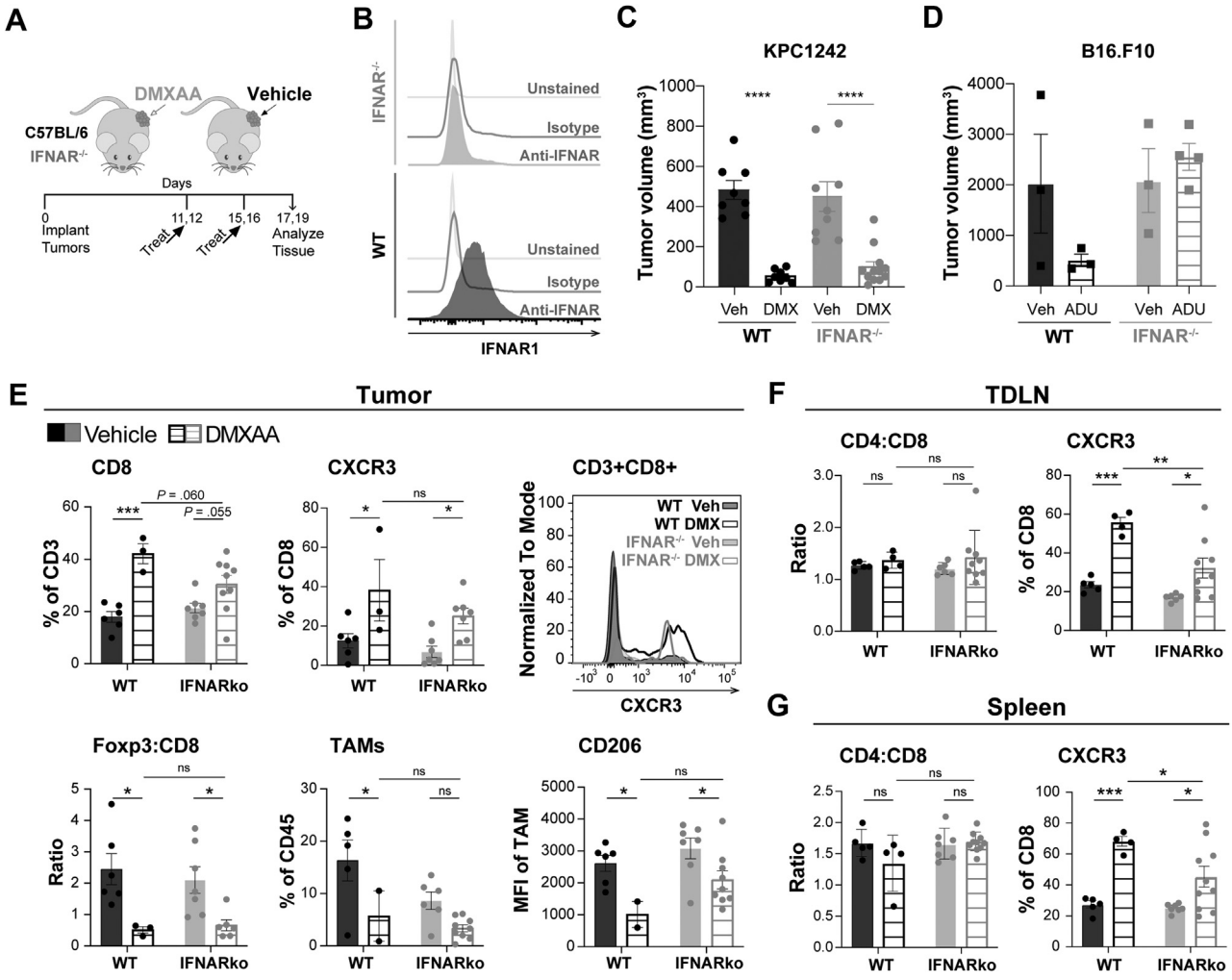

Figure 7. IFNAR signaling by pancreatic cancer cells promotes STING activated antitumor response. (*A*) C57BL/6 (wild-type [WT]) or IFNAR$^{-/-}$ mice were engrafted subcutaneously with single-flank KPC1242 PDA cells and treated with 450 μg DMXAA or vehicle control. (*B*) Validation of IFNAR$^{-/-}$ mouse model; representative flow cytometry histograms of IFNAR surface expression normalized to mode on splenocytes collected from WT or IFNAR$^{-/-}$ mice. (*C*) KPC1242 tumor volume at study end. (*D*) Subcutaneous B16.F10 melanoma tumor volume in response to ADU-S100 STING agonist treatment in WT or IFNAR$^{-/-}$ host mice. (*E–G*) Cellular immune profiles in the tumor (*E*), TDLNs (*F*), and spleen (*G*) of WT or IFNAR$^{-/-}$ mice. Error bars represent mean ± SEM. n = 4–10 from 2 independent experiments. ns, not significant. *$P < .05$, **$P < .01$, ***$P < .001$, ****$P < .0001$.

within tumor tissue and PDA cells treated with STING agonist revealed increased levels of immune-stimulatory molecules, including type I IFN–regulated T cell–attracting chemokines CXCL9 and CXCL10. IFNAR signaling by tumor cells was sufficient to drive contraction of PDA tumors in the absence of IFNAR signaling by accessory cells of the tumor microenvironment. Furthermore, we demonstrated for the first time that the antitumor effects and tumor infiltration of cytolytic T cells upon STING agonist treatment require CXCR3 expression. These data support a model in which STING activation induces tumor-intrinsic and tumor-extrinsic type I IFN signaling to drive the production of inflammatory cytokines and a physiologically relevant chemokine gradient of T cell–attracting chemokines to direct infiltration of effector T cells.

We tested the ability of local STING agonist injection into PDA tumors to generate widespread antitumor responses capable of acting at distal sites. Recent preclinical reports indicate that STING activation boosted preexisting antitumor immune responses in immunogenic melanoma, breast, and colon cancers to eradicate tumors at injected and contralateral sites.[17–19,40,41] However, the murine KPC implantation model recapitulates human PDA disease that lacks spontaneous antitumor responses. In this non-immunogenic model, effector CD8^{+} T cells were more abundant in tumors injected directly with STING agonists as well as in contralateral tumors not receiving treatment. Furthermore, STING agonist induced tumor antigen-specific T-cell activation at both sites and increased the frequency of cytolytic T cells within the draining lymph nodes of the injected and contralateral tumors, supporting a role for

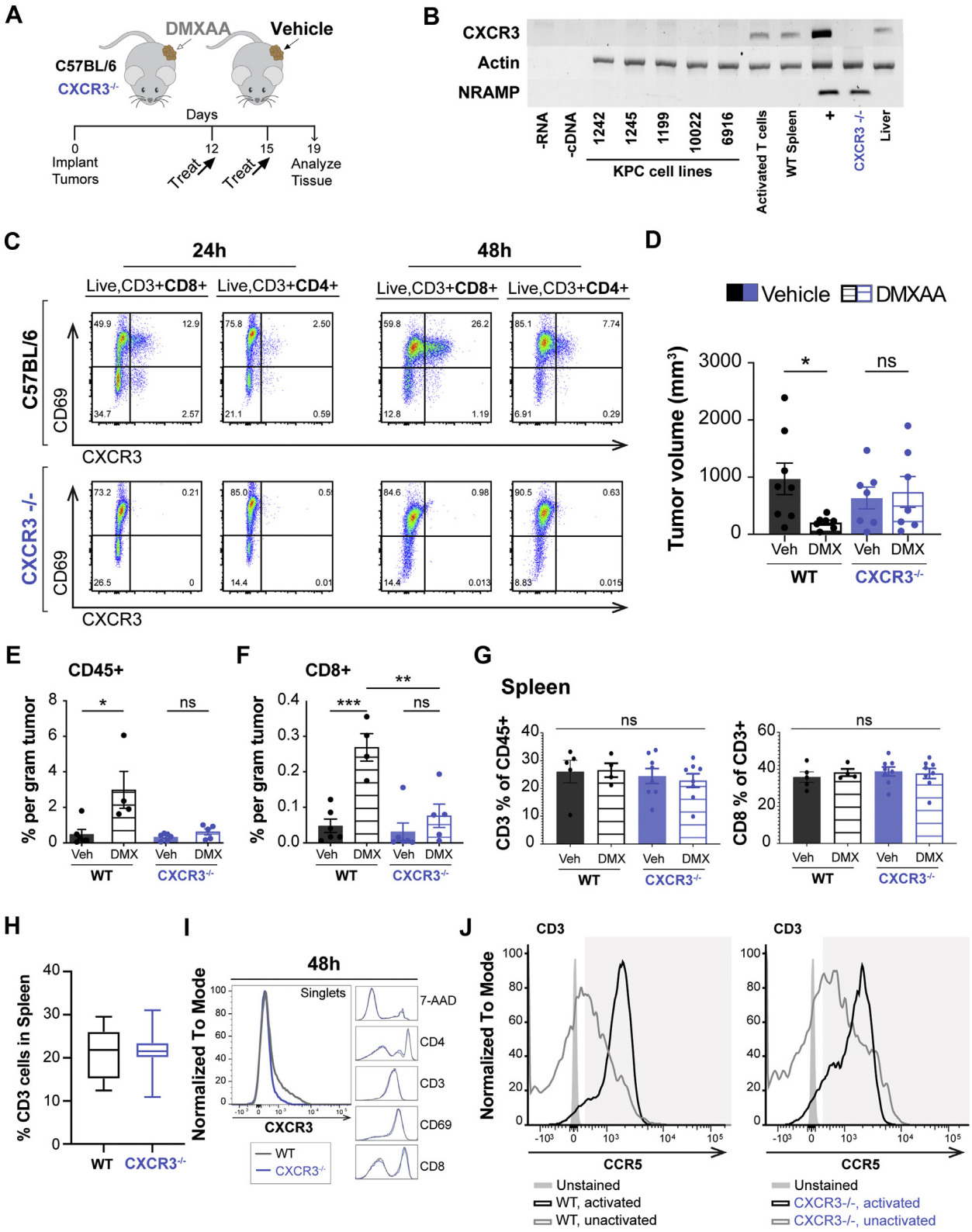

STING-mediated induction of systemic adaptive immunity. However, the potential contribution of systemic STING agonist distribution acting directly at distal PDA tumors cannot be overlooked. Indeed, a recent report indicates that different doses of STING agonist eradicate breast cancers through codependent mechanisms, with lower immunogenic doses stimulating antitumor T-cell expansion, whereas higher ablative doses promote highly inflammatory pathways, including tumor necrosis factor α signaling, at the expense of T-cell expansion.[19,42] In their dual-flank breast cancer model, local administration of ablative S100 doses resulted in immunogenic S100 levels in the contralateral

tumor, and both tumors shrank.[19] On the other hand, contralateral tumors progressed on administration of immunogenic doses,[19] illustrating the importance of both nonexclusive mechanisms of STING activation in long-term antitumor responses. Data from phase I clinical trials show that S100 absorption from intratumoral injection was rapid, reaching maximal plasma concentration within minutes, and has a circulation half-life of approximately 10–23 minutes. These data suggest that although S100 may achieve high local concentrations, its blood levels diminish rapidly. Moreover, the hypovascular nature of PDA tumors limits drug accessibility.[4,5] We postulate that the increase in tumor killing by TILs from STING agonist-injected and noninjected PDA tumors reflects the generation of local and systemic adaptive antitumor immunity. Induction of systemic antitumor immunity by STING agonist may provide a therapeutic avenue in the treatment of aggressive PDA such that local treatment of often more accessible metastatic lesions may enable control of visceral primary tumors and other nontreated metastatic lesions.

Prior reports have suggested that pattern recognition receptor signaling has paradoxical roles in PDA progression likely reflecting cell-type–specific signaling or pathway-specific signaling.[43–46] STING is a nearly ubiquitous pattern recognition receptor that stimulates production of type I IFNs during antiviral immune responses. Our data support this notion because each of the murine cell lines tested expressed the STING transcript. Type I IFNs have tumor-intrinsic and tumor-extrinsic antitumor properties.[24] Indeed, a recent report indicates that type I IFN signaling is suppressed in pancreatic cancers.[27] Furthermore, IFNγ-based chemoradiation provided long-term survival benefit in PDA patients, albeit with significant toxicity.[47] STING agonist-mediated contraction of immunogenic melanoma tumors was linked to dendritic cell IFNAR signaling, an example of extrinsic tumor control.[15] Our data showed that STING activation could regress IFNAR-responsive non-immunogenic PDA tumors engrafted to hosts with absent IFNAR signaling, supporting a role for tumor-intrinsic IFNAR signaling in the PDA response to STING agonist therapy. Moreover, human PDA cells expressing higher levels of IFNAR were more sensitive to IFNα/β-mediated antiproliferative and pro-apoptotic effects.[48,49] Although tumor-intrinsic IFNAR signaling activated local and systemic immune responses in our model, the lack of complete eradication suggests that tumor-extrinsic IFNAR signaling by additional cell types within the PDA tumor microenvironment may be required to unleash the full inflammatory effects of STING agonist. Alternatively, TBK1 activation by STING within PDA cells may act through IFNAR-independent mechanisms, because TBK1 also plays a critical role in induction of autophagy.[50] Autophagy has been shown in different model systems to paradoxically promote tumorigenesis or inhibit PDA progression. Thus, STING stimulation of TBK1-mediated autophagy is a potential IFNAR-independent process mediating its antitumor effects.

Intratumoral STING activation strongly induced inflammatory cytokine and chemokine production within PDA tumors, including CXCL9 and CXCL10. Although evidence suggests that these chemokine ligands mediate T-cell trafficking to and within melanoma tumors,[51,52] their roles and the establishment of the appropriate chemical gradients in fibrotic PDA tumors have not been shown. CXCL9 and CXCL10 are up-regulated by type I and type II IFN and engage their cognate receptor CXCR3 expressed nearly exclusively by activated effector T cells. Our data showed increased PDA-infiltrating $CXCR3^{+}CD8^{+}$ T-cell populations and tumor growth inhibition on STING activation in both wild-type and $IFNAR^{-/-}$ mice. PDA cells were identified as robust producers of CXCL10 in response to STING stimulation, indicating an important role for epithelial and immune cell chemokines in contributing to tumor infiltration of $CXCR3^{+}$ cells. The loss of this chemokine receptor resulted in a loss of STING agonist efficacy. Thus, CXCR3 appears to play an essential role in the antitumor response to STING agonist. Because elevated levels of CXCL9 and CXCL10 in the plasma of PDA patients significantly correlated with longer survival,[53] our data validate the potential for success for STING agonist therapy in human PDA disease.

STING agonist was effective as a single-agent therapy in a physiologically relevant model of pancreas cancer. Human PDAs often develop resistance to single agent therapeutics.[54,55] Suppressive myeloid populations interfere with therapeutic efficacy of checkpoint blockade inhibitors in murine PDA models.[56,57] STING-induced reprogramming of the myeloid immune compartment from suppressive-type TAMs into inflammatory-type TAMs[58] suggests that combining it with anti-PD1 may yield even greater anti-PDA responses as shown recently in colon cancer.[59] Here, 2 distinct STING agonists, including clinically relevant S100, were shown to modulate the immunologic landscape of locally injected tumors as well as tumors distal to the

Figure 8. (***See previous page***). **STING antitumor immune responses in CXCR3-deficient mice.** (*A*) Schematic treatment schedule for C57BL/6 (wild-type [WT]) or $CXCR3^{-/-}$ mice engrafted subcutaneously with KPC1242 PDA cells. (*B*) mRNA expression of CXCR3 in murine KPC cell lines, WT mouse spleen, or CD3/CD28-activated WT T cells. NRAMP non-coding region was amplified as a control for genomic DNA. +, WT mouse positive control. (*C*) Expression of CXCR3 and CD69 early activation marker on T cells derived from spleens of $CXCR3^{-/-}$ or WT mice measured by flow cytometry at 24 and 48 hours after activation. (*D*) Tumor volume from WT (*black bars*) and $CXCR3^{-/-}$ (*blue bars*) mice treated intratumorally with 450 μg DMXAA or vehicle control. (*E* and *F*) Cellular frequencies of tumor-infiltrating pan-leukocyte $CD45^{+}$ immune cells (*E*) and tumor-infiltrating $CD8^{+}$ cytolytic T cells (*F*). (*G*) Frequencies of $CD3^{+}$ or $CD8^{+}$ cells within spleens of PDA tumor-bearing WT or $CXCR3^{-/-}$ mice. (*H* and *I*) Within spleens of non–tumor-bearing WT or $CXCR3^{-/-}$ mice, an analysis of $CD3^{+}$ T cell frequencies (*H*) and additional cell-type frequencies and phenotypes (*I*). (*J*) Expression of CCR5, another surface chemokine on activated splenocytes, remains consistent between WT and $CXCR3^{-/-}$ mice. Error bars represent mean ± SEM. n = 4–8 mice from 2 independent experiments. ns, not significant. $^{*}P < .05$, $^{**}P < .01$, $^{***}P < .001$.

treated site. Our distal engraftment approach, which is used as a surrogate for disseminated cancer that is observed in more than 80% of human pancreatic cancer patients, suggests the translational potential for injecting STING agonist to one tumor site to promote immune activation in distal, untreated tumors. Thus, harnessing the power of the body's own defense system through exogenous activation of the STING pathway may be a viable therapeutic approach in the management of PDA.

Materials and Methods

All authors had access to the study data and had reviewed and approved the final manuscript.

Mouse Models and Cell Lines

Murine *LSL-KRas$^{G12D/+}$-LSL-Trp53$^{R172H/+}$-Pdx-1-Cre* (KPC) cells were maintained in high-glucose (4.5 g/mL) Dulbecco modified Eagle medium (DMEM) (Life Technologies Inc, Carlsbad, CA) supplemented with 10% (v/v) fetal bovine serum (Omega Scientific, Tarzana, CA) and 1X penicillin/streptomycin. Cell lines were authenticated annually using short tandem repeat profiling and mycoplasma-tested semiannually. The Institutional Animal Care and Use Committee at the Medical College of Wisconsin approved all animal studies (AUA000076). C57BL/6 mice were purchased from the Jackson Laboratory (Bar Harbor, ME). IFNAR$^{-/-}$ mice on C57BL/6 genetic background were originally obtained from the Sprent laboratory (Scripps Research Institute, La Jolla, CA).[60,61] CXCR3$^{-/-}$ mice (*B6.129P2-Cxcr3^{tm1Dgen}/J*) were obtained from the Jackson Laboratories. Six- to eight-week-old mice were implanted subcutaneously into one or both flanks with 2×10^5–1×10^6 syngeneic KPC cells and randomly assigned to treatment or control groups. Male mice were engrafted with KPC1242 cells, consistent with the sex from which the tumor cells were derived.[62] Experimental treatments were 450 μg 5,6-dimethyl-9-oxo-9*H*-xanthene-4-acetic acid (DMXAA) (Tocris, Minneapolis, MN) in 50 μL of 0.67% (v/v) $NaHCO_3$–phosphate-buffered saline (PBS) or titrated doses of ADU-S100 (MedChemExpress, Monmouth Junction, NJ) in 50 μL sterile water. Mice were treated with intratumoral injections into a single flank after tumors had established on days 9–12. Tumor area (mm^2) was calculated by using the formula length $\times$ width, as measured by calipers along the cranial-caudal and ventral-dorsal axes. After tumor excision, tumor volume (mm^3) using the formula length $\times$ width $\times$ depth was measured. Reagents are listed in Table 1.

Tissue Dissociation

After euthanasia, tumors were excised and collected in cold PBS with 0.5% (w/v) bovine serum albumin on ice. Tumors were minced, transferred to gentleMACS C-Tubes, and enzymatically dissociated in DMEM with Mouse Tumor Dissociation kit reagents (Miltenyi Biotec, San Diego, CA). Samples were digested by using the gentleMACS Dissociator and incubated at 37°C for 40 minutes, followed by serial filtration through 70-μm and 30-μm strainers. After washing in PBS, the resultant single-cell suspension was used immediately for flow cytometry analyses.

Immune Monitoring

Cell suspensions from tumor, spleen, and TDLNs were stained with Live/Dead Fixable Aqua Dead Cell Stain (Thermo Fisher, Waltham, MA) in PBS, followed by Fc receptor blocking with anti-CD16/32 antibody (BioXCell, Lebanon, NH) and multiparametric extracellular surface antigen staining in PBS and 0.5% (w/v) bovine serum albumin. Cells were then fixed with PBS/1% (w/v) paraformaldehyde or permeabilized for intracellular staining using Foxp3/Transcription Factor Staining Buffer (eBioscience, San Diego, CA), followed by intracellular antigen staining. Fluorochrome-labeled antibodies are listed in Table 2. Super Bright Staining Buffer was used to minimize nonspecific interactions between fluorochrome labels (Invitrogen, Carlsbad, CA). Cell populations were detected by using flow cytometry as shown in representative gating strategies detailed in Figure 1*E* and *F*. Samples were acquired on the BD LSRFortessa X-20. Data were analyzed by using FlowJo software (10.6.1; Becton Dickinson, Franklin Lakes, NJ). Cell populations of interest were

Table 1. Key Reagents and Chemicals

Reagent	Manufacturer	Catalog no.
DMEM	Gibco	11965084
Fetal bovine serum	Omega	FB-12
DMXAA	Tocris	5601
ADU-S100	MedChemExpress	HY-12885B
Mouse Tumor Dissociation Kit	Miltenyi	130-096-730
Super Bright Staining Buffer	Invitrogen	SB-4400-42
Live/Dead Aqua Fixable Dead Cell Stain	Thermo Fisher	L34957
FcR Blocking anti-CD16/32, clone 2.4G2	BioXCell	BE0307
Protease inhibitors	Sigma	539134
Foxp3 Transcription Factor Staining Buffer	eBioscience	00-5523-00
RNeasy Kit	Qiagen	74104
DNase	Ambion	AM1906

Table 2. Flow Cytometry Antibodies

Target antigen	Fluorochrome	Clone	Host isotype	Manufacturer	Catalog no.
CD45	Alexa Fluor700	30-F11	Rat IgG2b, κ	eBioscience	56-0451
CD3	APC-eF780	17A2	Hamster IgG	eBioscience	47-0032
CD4	APC	GK1.5	Rat IgG2b, κ	eBioscience	17-0041
CD8	BUV395	53-6.7	Rat IgG2a, κ	BD Bioscience	563786
CD11b	SB600	M1/70	Rat IgG2b, κ	eBioscience	63-0112
CD11c	PE-eFluor610	N418	Hamster IgG	eBioscience	61-0114
CD19	PE-cyanine7	eBio1D3	Rat IgG2a, κ	eBioscience	25-0193
CD62L	SuperBright702	MEL-14	Rat IgG2a, κ	eBioscience	67-0621
CD69	SuperBright436	H1.2F3	Hamster IgG	eBioscience	62-0691
CXCR3	PE	CXCR3-173	Hamster IgG	eBioscience	12-1831
CD335/NKp46	FITC	29A1.4	Rat IgG2a, κ	eBioscience	11-3351
Granzyme B	FITC	GB11	Mouse IgG1, κ	BioLegend	515403
CD279 (PD-1)	PE-Cy7	J43	Hamster IgG	eBioscience	25-9985
FoxP3	APC	FJK-16s	Rat IgG2a, κ	eBioscience	17-5773
CD103	APC	2E7	Hamster IgG	eBioscience	17-1031
CD206	PE-Cy7	MR6F3	Rat IgG2b, κ	eBioscience	25-2061
F4/80	SB702	BM8	Rat IgG2a, κ	eBioscience	67-4801
Ly-6C	PE	HK1.4	Rat IgG2c, κ	eBioscience	12-5932
Ly-6G	FITC	IA8	Rat IgG2a, κ	eBioscience	11-9668
MHC Class II	eFluor	M5/114.15.2	Rat IgG2b, κ	eBioscience	61-0114
IFNAR	PE	MAR1-5A3	Mouse IgG1, κ	BioLegend	12-7311
Isotype control IgG1κ.	PE	MOPC-21	Mouse IgG1, κ	BioLegend	400111

Ig, immunoglobulin.

normalized to the percent of total cells from the collected single-cell suspension or of parent gate populations to correct for variability in tumor regression after treatment with STING agonist.

Cytokine/Chemokine Array

After euthanasia, tumors were excised and collected in cold homogenate buffer (20 mmol/L Tris-HCl pH 7.9, 0.5% [v/v] Tween, 150 mmol/L NaCl, and 1:100 protease inhibitors [Sigma Chemical Co, St Louis, MO]). Tumors were weighed and minced, and the tumor was homogenized by using gentleMACS M-Tubes and Dissociator, centrifuged at 4500*g*, and supernatant was collected and frozen. PDA homogenates were analyzed by using the Mouse Cytokine Array/Chemokine Array 44-plex to detect secreted proteins on the basis of binding to fluorescently coded polystyrene beads labeled with capture antibody (Eve Technologies, Calgary, Canada).

Table 3. RT-PCR Primer Sequences

Target	Forward primer (5′ → 3′)	Reverse primer (5′ → 3′)
Mx1	AGCTAGACAGAGCAAACCAAGCCA	TCCCTGAAGCAGACACAGCTGAAA
Mx2	AGCAGAGTGACACAAGCGAGAAGA	AGCCCTTCTGTCCCTGAATCACAA
mSTING	GTTGATCTTACCAGGGCTCCAGGC	AGGCGGCAGTTATTTCGAGACTCG
Cxcr3	GTGGCTGCTGTGCTACTGAGTCAGC	GCATTGAGGCGCTGATCGTAGTTGGC
β-actin	TGACGGGGTCACCCACACTGTGCCCATCTA	CTAGAAGCATTGCGGTGGACGATGGAGGG
Nramp	CAGGAAGGACCAGAAATCGGA	TGAGTAAGAGTGGGAACCCACG

NOTE. Conditions: Mx1 and Mx2 were amplified by using 35-cycle PCR reactions (45 seconds at 94°C, 30 seconds at 65°C, 60 seconds at 72°C). mSTING transcript expression was amplified by using 30-cycle PCR reaction (60 seconds at 94°C, 2.5 minutes at 68°C). CXCR3 transcript expression was amplified by using 30-cycle PCR reaction (30 seconds at 94°C, 2 minutes 30 seconds at 62°C, 30 seconds at 72°C). Mouse beta-actin mRNA and genomic NRAMP were amplified by using 30-cycle PCR reaction (30 seconds at 94°C, 30 seconds at 62°C, 30 seconds at 72°C).

RT-PCR

RNA was isolated from cells by using the RNeasy kit (Qiagen, Thermo Fisher, Waltham, MA) and treated with DNase (Ambion, Thermo Fisher). After nanodrop inspection of RNA quality and yield, total RNA was converted to cDNA using Superscript RT III. Transcript expression was measured by using RT-PCR, with the primers and conditions listed in Table 3.

T Cell Killing Assay

$CD8^+$ TILs were isolated and expanded ex vivo from dissociated injected or contralateral PDA tumors from DMXAA-treated mice as described previously.[28] Target PDA KPC1242 cells stably expressing mCherry were cultured overnight in a 96-well plate. Expanded TILs were incubated with KPC cells at a target-to-effector ratio of 1:10 along with 5 μmol/L apoptosis reagent caspase-3/7, and cell killing was measured by using real-time IncuCyte S3 (Essen BioScience, Ann Arbor, MI) imaging. Mean green fluorescence values from TILs alone in culture were subtracted from co-culture wells at corresponding time points.

Statistical Analyses

Statistical analyses were performed by using Prism 8.0 software or R version 3.6.0. Power analysis was performed by using an alpha error probability of 0.05 and a power level of 0.8 to select rigorous sample sizes for individual experiments. Unpaired sample comparisons between 2 groups were analyzed by Student t test when data were normally distributed with equal variances of the groups or by Mann-Whitney test when parametric test conditions were violated. Three or more independent groups were compared by using one-way analysis of variance with Tukey's honestly significant difference test for multiple comparisons. When 2 independent variables were analyzed, a two-way analysis of variance with the Sidak's test for multiple comparisons was used to calculate significance values. A log-rank Mantel-Cox test was used to compare differences in survival curves between experimental groups.

References

1. Siegel RL, Miller KD, Jemal A. Cancer statistics, 2020. CA Cancer J Clin 2020;70:7–30.
2. Adamska A, Domenichini A, Falasca M. Pancreatic ductal adenocarcinoma: current and evolving therapies. IJMS 2017;18:1338.
3. Vincent A, Herman J, Schulick R, Hruban RH, Goggins M. Pancreatic cancer. Lancet 2011; 378:607–620.
4. Olive KP, Jacobetz MA, Davidson CJ, Gopinathan A, McIntyre D, Honess D, Madhu B, Goldgraben MA, Caldwell ME, Allard D, Frese KK, Denicola G, Feig C, Combs C, Winter SP, Ireland-Zecchini H, Reichelt S, Howat WJ, Chang A, Dhara M, Wang L, Rückert F, Grützmann R, Pilarsky C, Izeradjene K, Hingorani SR, Huang P, Davies SE, Plunkett W, Egorin M, Hruban RH, Whitebread N, McGovern K, Adams J, Iacobuzio-Donahue C, Griffiths J, Tuveson DA. Inhibition of Hedgehog signaling enhances delivery of chemotherapy in a mouse model of pancreatic cancer. Science 2009; 324:1457–1461.
5. Provenzano PP, Cuevas C, Chang AE, Goel VK, Hoff Von DD, Hingorani SR. Enzymatic targeting of the stroma ablates physical barriers to treatment of pancreatic ductal adenocarcinoma. Cancer Cell 2012;21:418–429.
6. Beatty GL, Winograd R, Evans RA, Long KB, Luque SL, Lee JW, Clendenin C, Gladney WL, Knoblock DM, Guirnalda PD, Vonderheide RH. Exclusion of T cells from pancreatic carcinomas in mice is regulated by Ly6Clow F4/80+ extratumoral macrophages. Gastroenterology 2015;149:201–210.
7. Brahmer JR, Tykodi SS, Chow LQM, Hwu W-J, Topalian SL, Hwu P, Drake CG, Camacho LH, Kauh J, Odunsi K, Pitot HC, Hamid O, Bhatia S, Martins R, Eaton K, Chen S, Salay TM, Alaparthy S, Grosso JF, Korman AJ, Parker SM, Agrawal S, Goldberg SM, Pardoll DM, Gupta A, Wigginton JM. Safety and activity of anti-PD-L1 antibody in patients with advanced cancer. N Engl J Med 2012;366:2455–2465.
8. Catenacci DVT, Junttila MR, Karrison T, Bahary N, Horiba MN, Nattam SR, Marsh R, Wallace J, Kozloff M, Rajdev L, Cohen D, Wade J, Sleckman B, Lenz H-J, Stiff P, Kumar P, Xu P, Henderson L, Takebe N, Salgia R, Wang X, Stadler WM, de Sauvage FJ, Kindler HL. Randomized phase Ib/II study of gemcitabine plus placebo or vismodegib, a Hedgehog pathway inhibitor, in patients with metastatic pancreatic cancer. J Clin Oncol 2015; 33:4284–4292.
9. Sharma P, Allison JP. Immune checkpoint targeting in cancer therapy: toward combination strategies with curative potential. Cell 2015;161:205–214.
10. Clark CE, Hingorani SR, Mick R, Combs C, Tuveson DA, Vonderheide RH. Dynamics of the immune reaction to pancreatic cancer from inception to invasion. Cancer Res 2007;67:9518–9527.
11. Stromnes IM, Hingorani SR, Hulbert A, Greenberg PD, Pierce RH. T-cell localization, activation, and clonal expansion in human pancreatic ductal adenocarcinoma. Cancer Immunol Res 2017;5:978–991.
12. Blando J, Sharma A, Higa MG, Zhao H, Vence L, Yadav SS, Kim J, Sepulveda AM, Sharp M, Maitra A, Wargo J, Tetzlaff M, Broaddus R, Katz MHG, Varadhachary GR, Overman M, Wang H, Yee C, Bernatchez C, Iacobuzio-Donahue C, Basu S, Allison JP, Sharma P. Comparison of immune infiltrates in melanoma and pancreatic cancer highlights VISTA as a potential target in pancreatic cancer. Proc Natl Acad Sci USA 2019;116:1692–1697.
13. Chen DS, Mellman I. Oncology meets immunology: the cancer-immunity cycle. Immunity 2013;39:1–10.
14. Ene-Obong A, Clear AJ, Watt J, Wang J, Fatah R, Riches JC, Marshall JF, Chin-Aleong J, Chelala C, Gribben JG, Ramsay AG, Kocher HM. Activated pancreatic stellate cells sequester CD8+ T cells to reduce their infiltration of the juxtatumoral compartment of pancreatic ductal adenocarcinoma. Gastroenterology 2013;145:1121–1132.

15. Woo S-R, Fuertes MB, Corrales L, Spranger S, Furdyna MJ, Leung MYK, Duggan R, Wang Y, Barber GN, Fitzgerald KA, Alegre M-L, Gajewski TF. STING-dependent cytosolic DNA sensing mediates innate immune recognition of immunogenic tumors. Immunity 2014;41:830–842.
16. Woo S-R, Corrales L, Gajewski TF. Innate immune recognition of cancer. Annu Rev Immunol 2015; 33:445–474.
17. Corrales L, Glickman LH, McWhirter SM, Kanne DB, Sivick KE, Katibah GE, Woo S-R, Lemmens E, Banda T, Leong JJ, Metchette K, Dubensky TW Jr, Gajewski TF. Direct activation of STING in the tumor microenvironment leads to potent and systemic tumor regression and immunity. Cell Reports 2015;11:1018–1030.
18. Demaria O, De Gassart A, Coso S, Gestermann N, Di Domizio J, Flatz L, Gaide O, Michielin O, Hwu P, Petrova TV, Martinon F, Modlin RL, Speiser DE, Gilliet M. STING activation of tumor endothelial cells initiates spontaneous and therapeutic antitumor immunity. Proc Natl Acad Sci USA 2015;112:15408–15413.
19. Sivick KE, Desbien AL, Glickman LH, Reiner GL, Corrales L, Surh NH, Hudson TE, Vu UT, Francica BJ, Banda T, Katibah GE, Kanne DB, Leong JJ, Metchette K, Bruml JR, Ndubaku CO, McKenna JM, Feng Y, Zheng L, Bender SL, Cho CY, Leong ML, van Elsas A, Dubensky TW Jr, McWhirter SM. Magnitude of therapeutic STING activation determines CD8+ T cell-mediated anti-tumor immunity. Cell Reports 2018; 25:3074–3075.
20. Ishikawa H, Barber GN. STING is an endoplasmic reticulum adaptor that facilitates innate immune signalling. Nature [Internet] 2008;455 2008:674–678. Available from: http://www.nature.com/doifinder/10.1038/nature07317.
21. Ishikawa H, Ma Z, Barber GN. STING regulates intracellular DNA-mediated, type I interferon-dependent innate immunity. Nature 2009;461:788–792.
22. Ishikawa H, Barber GN. The STING pathway and regulation of innate immune signaling in response to DNA pathogens. Cell Mol Life Sci 2011;68:1157–1165.
23. Isaacs A, Lindenmann J. Virus interference: I—the interferon. Proc R Soc Lond B Biol Sci 1957;147:258–267.
24. Bekisz J, Baron S, Balinsky C, Morrow A, Zoon KC. Antiproliferative properties of type I and type II interferon. Pharmaceuticals (Basel) 2010;3:994–1015.
25. Fuertes MB, Kacha AK, Kline J, Woo S-R, Kranz DM, Murphy KM, Gajewski TF. Host type I IFN signals are required for antitumor CD8+ T cell responses through CD8{alpha}+ dendritic cells. J Exp Med 2011; 208:2005–2016.
26. Dunn GP, Bruce AT, Sheehan KCF, Shankaran V, Uppaluri R, Bui JD, Diamond MS, Koebel CM, Arthur C, White JM, Schreiber RD. A critical function for type I interferons in cancer immunoediting. Nat Immunol 2005; 6:722–729.
27. Muthalagu N, Monteverde T, Raffo-Iraolagoitia X, Wiesheu R, Whyte D, Hedley A, Laing S, Kruspig B, Upstill-Goddard R, Shaw R, Neidler S, Rink C, Karim SA, Gyuraszova K, Nixon C, Clark W, Biankin AV, Carlin LM, Coffelt SB, Sansom OJ, Morton JP, Murphy DJ. Repression of the type I interferon pathway underlies MYC- and KRAS-dependent evasion of NK and B cells in pancreatic ductal adenocarcinoma. Cancer Discov 2020; 10:872–887.
28. Jing W, McAllister D, Vonderhaar EP, Palen K, Riese MJ, Gershan J, Johnson BD, Dwinell MB. STING agonist inflames the pancreatic cancer immune microenvironment and reduces tumor burden in mouse models. Journal for Immunotherapy of Cancer 2019;7:115.
29. Woo S-R, Corrales L, Gajewski TF. The STING pathway and the T cell-inflamed tumor microenvironment. Trends in Immunology 2015;36:250–256.
30. Lara PN, Douillard J-Y, Nakagawa K, Pawel von J, McKeage MJ, Albert I, Losonczy G, Reck M, Heo D-S, Fan X, Fandi A, Scagliotti G. Randomized phase III placebo-controlled trial of carboplatin and paclitaxel with or without the vascular disrupting agent vadimezan (ASA404) in advanced non-small-cell lung cancer. J Clin Oncol 2011;29:2965–2971.
31. Conlon J, Burdette DL, Sharma S, Bhat N, Thompson M, Jiang Z, Rathinam VAK, Monks B, Jin T, Xiao TS, Vogel SN, Vance RE, Fitzgerald KA. Mouse, but not human STING, binds and signals in response to the vascular disrupting agent 5,6-dimethylxanthenone-4-acetic acid. J Immunol 2013;190:5216–5225.
32. Lee JW, Komar CA, Bengsch F, Graham K, Beatty GL. Genetically engineered mouse models of pancreatic cancer: the KPC model (LSL-Kras G12D/+;LSL-Trp53 R172H/+;Pdx-1-Cre), its variants, and their application in immuno-oncology drug discovery. Hoboken, NJ: John Wiley & Sons, Inc, 2016.
33. Su T, Zhang Y, Valerie K, Wang X-Y, Lin S, Zhu G. STING activation in cancer immunotherapy. Theranostics 2019; 9:7759–7771.
34. Mimura K, Teh JL, Okayama H, Shiraishi K, Kua L-F, Koh V, Smoot DT, Ashktorab H, Oike T, Suzuki Y, Fazreen Z, Asuncion BR, Shabbir A, Yong W-P, So J, Soong R, Kono K. PD-L1 expression is mainly regulated by interferon gamma associated with JAK-STAT pathway in gastric cancer. Cancer Science 2018; 109:43–53.
35. Balachandran VP, Łuksza M, Zhao JN, Makarov V, Moral JA, Remark R, Herbst B, Askan G, Bhanot U, Senbabaoglu Y, Wells DK, Cary CIO, Grbovic-Huezo O, Attiyeh M, Medina B, Zhang J, Loo J, Saglimbeni J, Abu-Akeel M, Zappasodi R, Riaz N, Smoragiewicz M, Kelley ZL, Basturk O, Gönen M, Levine AJ, Allen PJ, Fearon DT, Merad M, Gnjatic S, Iacobuzio-Donahue CA, Wolchok JD, DeMatteo RP, Chan TA, Greenbaum BD, Merghoub T, Leach SD. Identification of unique neoantigen qualities in long-term survivors of pancreatic cancer. Nature 2017;551:512–516.
36. Diamond MS, Kinder M, Matsushita H, Mashayekhi M, Dunn GP, Archambault JM, Lee H, Arthur CD, White JM, Kalinke U, Murphy KM, Schreiber RD. Type I interferon is selectively required by dendritic cells for immune rejection of tumors. J Exp Med 2011; 208:1989–2003.
37. Jablonska J, Leschner S, Westphal K, Lienenklaus S, Weiss S. Neutrophils responsive to endogenous IFN-

beta regulate tumor angiogenesis and growth in a mouse tumor model. J Clin Invest 2010; 120:1151–1164.
38. Dwinell MB, Lügering N, Eckmann L, Kagnoff MF. Regulated production of interferon-inducible T-cell chemoattractants by human intestinal epithelial cells. Gastroenterology 2001;120:49–59.
39. Roy I, Boyle KA, Vonderhaar EP, Zimmerman NP, Gorse E, Mackinnon AC, Hwang RF, Franco-Barraza J, Cukierman E, Tsai S, Evans DB, Dwinell MB. Cancer cell chemokines direct chemotaxis of activated stellate cells in pancreatic ductal adenocarcinoma. Lab Invest 2017; 97:302–317.
40. Ager CR, Reilley MJ, Nicholas C, Bartkowiak T, Jaiswal AR, Curran MA. Intratumoral STING activation with T-cell checkpoint modulation generates systemic antitumor immunity. Cancer Immunol Res 2017; 5:676–684.
41. Foote JB, Kok M, Leatherman JM, Armstrong TD, Marcinkowski BC, Ojalvo LS, Kanne DB, Jaffee EM, Dubensky TWJ, Emens LA. A STING agonist given with OX40 receptor and PD-L1 modulators primes immunity and reduces tumor growth in tolerized mice. Cancer Immunol Res 2017;5:468–479.
42. Baird JR, Friedman D, Cottam B, Dubensky TW Jr, Kanne DB, Bambina S, Bahjat K, Crittenden MR, Gough MJ. Radiotherapy combined with novel STING-targeting oligonucleotides results in regression of established tumors. Cancer Res 2016;76:50–61.
43. Ikebe M, Kitaura Y, Nakamura M, Tanaka H, Yamasaki A, Nagai S, Wada J, Yanai K, Koga K, Sato N, Kubo M, Tanaka M, Onishi H, Katano M. Lipopolysaccharide (LPS) increases the invasive ability of pancreatic cancer cells through the TLR4/MyD88 signaling pathway. J Surg Oncol 2009;100:725–731.
44. Ochi A, Nguyen AH, Bedrosian AS, Mushlin HM, Zarbakhsh S, Barilla R, Zambirinis CP, Fallon NC, Rehman A, Pylayeva-Gupta Y, Badar S, Hajdu CH, Frey AB, Bar-Sagi D, Miller GW. MyD88 inhibition amplifies dendritic cell capacity to promote pancreatic carcinogenesis via Th2 cells. J Exp Med 2012; 209:1671–1687.
45. Duewell P, Steger A, Lohr H, Bourhis H, Hoelz H, Kirchleitner SV, Stieg MR, Grassmann S, Kobold S, Siveke JT, Endres S, Schnurr M. RIG-I-like helicases induce immunogenic cell death of pancreatic cancer cells and sensitize tumors toward killing by CD8(+) T cells. Cell Death Differ 2014;21:1825–1837.
46. Zambirinis CP, Levie E, Nguy S, Avanzi A, Barilla R, Xu Y, Seifert L, Daley D, Greco SH, Deutsch M, Jonnadula S, Torres-Hernandez A, Tippens D, Pushalkar S, Eisenthal A, Saxena D, Ahn J, Hajdu C, Engle DD, Tuveson D, Miller GW. TLR9 ligation in pancreatic stellate cells promotes tumorigenesis. J Exp Med 2015; 212:2077–2094.
47. Rocha FG, Hashimoto Y, Traverso LW, Dorer R, Kozarek R, Helton WS, Picozzi VJ. Interferon-based adjuvant chemoradiation for resected pancreatic head cancer: long-term follow-up of the Virginia Mason protocol. Ann Surg 2016;263:376–384.
48. Vitale G, van Eijck CHJ, van Koetsveld Ing PM, Erdmann JI, Speel EJM, van der Wansem Ing K, Mooij DM, Colao A, Lombardi G, Croze E, Lamberts SWJ, Hofland LJ. Type I interferons in the treatment of pancreatic cancer: mechanisms of action and role of related receptors. Ann Surg 2007; 246:259–268.
49. Booy S, van Eijck CHJ, Dogan F, van Koetsveld PM, Hofland LJ. Influence of type-I interferon receptor expression level on the response to type-I interferons in human pancreatic cancer cells. J Cell Mol Med 2014; 18:492–502.
50. Ahmad L, Mashbat B, Leung C, Brookes C, Hamad S, Krokowski S, Shenoy AR, Lorenzo L, Levin M, O'Hare P, Zhang S-Y, Casanova J-L, Mostowy S, Sancho-Shimizu V. Human TANK-binding kinase 1 is required for early autophagy induction upon herpes simplex virus 1 infection. J Allergy Clin Immunol 2019;143:765–767.
51. Kunz M, Toksoy A, Goebeler M, Engelhardt E, Bröcker E, Gillitzer R. Strong expression of the lymphoattractant C-X-C chemokine Mig is associated with heavy infiltration of T cells in human malignant melanoma. J Pathol 1999; 189:552–558.
52. Harlin H, Meng Y, Peterson AC, Zha Y, Tretiakova M, Slingluff C, McKee M, Gajewski TF. Chemokine expression in melanoma metastases associated with CD8+ T-cell recruitment. Cancer Res 2009;69:3077–3085.
53. Qian L, Yu S, Yin C, Zhu B, Chen Z, Meng Z, Wang P. Plasma IFN-γ-inducible chemokines CXCL9 and CXCL10 correlate with survival and chemotherapeutic efficacy in advanced pancreatic ductal adenocarcinoma. Pancreatology 2019;19:340–345.
54. Conroy T, Desseigne F, Ychou M, Bouche O, Guimbaud R, Becouarn Y, Adenis A, Raoul JL, Gourgou-Bourgade S, la Fouchardiere de C, Bennouna J, Bachet JB, Khemissa-Akouz F, Pere-Verge D, Delbaldo C, Assenat E, Chauffert B, Michel P, Montoto-Grillot C, Ducreux M, Groupe Tumeurs Digestives of U, Intergroup P. FOLFIRINOX versus gemcitabine for metastatic pancreatic cancer. N Engl J Med 2011; 364:1817–1825.
55. Tsai S, Christians KK, Ritch PS, George B, Khan AH, Erickson B, Evans DB. Multimodality therapy in patients with borderline resectable or locally advanced pancreatic cancer: importance of locoregional therapies for a systemic disease. J Oncol Pract 2016;12:915–923.
56. Beatty GL, Chiorean EG, Fishman MP, Saboury B, Teitelbaum UR, Sun W, Huhn RD, Song W, Li D, Sharp LL, Torigian DA, O'Dwyer PJ, Vonderheide RH. CD40 agonists alter tumor stroma and show efficacy against pancreatic carcinoma in mice and humans. Science 2011;331:1612–1616.
57. Zhang Y, Velez-Delgado A, Mathew E, Li D, Mendez FM, Flannagan K, Rhim AD, Simeone DM, Beatty GL, Pasca di Magliano M. Myeloid cells are required for PD-1/PD-L1 checkpoint activation and the establishment of an immunosuppressive environment in pancreatic cancer. Gut 2017;66:124–136.
58. Downey CM, Aghaei M, Schwendener RA, Jirik FR. DMXAA causes tumor site-specific vascular

disruption in murine non-small cell lung cancer, and like the endogenous non-canonical cyclic dinucleotide STING agonist, 2′3′-cGAMP, induces M2 macrophage repolarization. PLoS One 2014;9:e99988–14.

59. Kim C, Kim W, Han Y, Kim J, Chon H. Cancer immunotherapy with STING agonist and PD-1 immune checkpoint inhibitor effectively suppresses peritoneal carcinomatosis of colon cancer. Ann Oncol 2019;30-(Suppl 4):iv35.
60. Grayson MH, Cheung D, Rohlfing MM, Kitchens R, Spiegel DE, Tucker J, Battaile JT, Alevy Y, Yan L, Agapov E, Kim EY, Holtzman MJ. Induction of high-affinity IgE receptor on lung dendritic cells during viral infection leads to mucous cell metaplasia. J Exp Med 2007;204:2759–2769.
61. Mboko WP, Rekow MM, Ledwith MP, Lange PT, Schmitz KE, Anderson S, Tarakanova VL. Interferon regulatory factor 1 and type I interferon cooperate to control acute gammaherpesvirus infection. J Virol 2017;91:2715.
62. Engle DD, Tiriac H, Rivera KD, Pommier A, Whalen S, Oni TE, Alagesan B, Lee EJ, Yao MA, Lucito MS, Spielman B, Da Silva B, Schoepfer C, Wright K, Creighton B, Afinowicz L, Yu KH, Grützmann R, Aust D, Gimotty PA, Pollard KS, Hruban RH, Goggins MG, Pilarsky C, Park Y, Pappin DJ, Hollingsworth MA, Tuveson DA. The glycan CA19-9 promotes pancreatitis and pancreatic cancer in mice. Science 2019;364:1156–1162.

Received August 26, 2020. Accepted January 26, 2021.

Correspondence
Address correspondence to: Michael B. Dwinell, PhD, Medical College of Wisconsin, Department of Microbiology and Immunology, 8701 Watertown Plank Road, Milwaukee, Wisconsin 53226. e-mail: mdwinell@mcw.edu; fax: (414) 955-6535.

Acknowledgments
The authors thank Weiqing Jing, PhD, Versiti Blood Research Institute, and Katie Palen, Cell Therapy Labs, Medical College of Wisconsin, for protocol development and optimization. They thank Douglas Evans, MD, and Susan Tsai, MD, MS, in the Department of Surgery and the LaBahn Pancreatic Cancer Program for their continued enthusiastic support and discussions on the detection, pathophysiology, and treatment of pancreatic cancer. The authors acknowledge the instrumental help, advice, and guidance of Matthew Riese, MD, PhD, who died suddenly after an acute illness. They are forever grateful for his help and will deeply miss his keen insights, steady guidance, and ready mentorship.

CRediT Authorship Contributions

Emily P. Vonderhaar, PhD (Conceptualization: Equal; Formal analysis: Lead; Investigation: Lead; Methodology: Lead; Visualization: Equal; Writing – original draft: Lead; Writing – review & editing: Equal)

Nicholas S. Barnekow, BS (Formal analysis: Supporting; Investigation: Supporting; Methodology: Supporting)

Donna McAllister, BS (Formal analysis: Supporting; Investigation: Supporting; Methodology: Supporting; Visualization: Equal; Writing – review & editing: Supporting)

Laura McOlash, BS (Formal analysis: Supporting; Investigation: Supporting; Visualization: Supporting)

Mahmoud Abu Eid, BS (Formal analysis: Supporting; Investigation: Supporting; Methodology: Equal; Visualization: Supporting; Writing – review & editing: Supporting)

Matthew J. Riese, MD, PhD (Conceptualization: Supporting; Formal analysis: Supporting; Methodology: Supporting; Resources: Supporting; Visualization: Supporting; Writing – review & editing: Supporting)

Vera L. Tarakanova, PhD (Conceptualization: Supporting; Investigation: Supporting; Methodology: Supporting; Resources: Supporting; Writing – review & editing: Supporting)

Bryon D. Johnson, PhD (Conceptualization: Supporting; Formal analysis: Equal; Funding acquisition: Supporting; Investigation: Supporting; Methodology: Supporting; Resources: Supporting; Writing – review & editing: Equal)

Michael B. Dwinell, PhD (Conceptualization: Equal; Formal analysis: Equal; Funding acquisition: Lead; Project administration: Lead; Resources: Lead; Supervision: Lead; Visualization: Equal; Writing – original draft: Supporting; Writing – review & editing: Lead)

Conflicts of interest
This author discloses the following: M.B.D. is a co-founder and has ownership interests in Protein Foundry, LLC and Xlock Bioscience LLC. The remaining authors disclose no conflicts.

Funding
Supported in part by grants from the NCI U01 CA178960 and R01 CA226279 to M.B.D and philanthropic support from the Advancing a Healthier Wisconsin Endowment and the Bobbie Nick Voss Charitable Foundation. E.P.V is a member of the Medical Scientist Training Program at MCW, which is partially supported by a training grant from NIGMS T32 GM080202. E.P.V was supported by the Clinical & Translational Science Institute of Southeast Wisconsin and the NCATS, TL1 TR001437. The content is solely the responsibility of the authors and does not necessarily represent the official views of the NIH. Funding agencies played no role in the study design, data collection, analysis, or interpretation.